

## ON MULTISCALE ACCELERATION STATISTICS IN ROTATING AND SHEARED HOMOGENEOUS TURBULENCE

**Frank G. Jacobitz**

Mechanical Engineering Program  
University of San Diego  
5998 Alcalá Park, San Diego, California 92110, USA  
jacobitz@sandiego.edu

**Kai Schneider**

M2P2-CNRS & CMI  
Aix-Marseille Université  
38 rue Joliot-Curie, 13453 Marseille Cedex 13, France  
kschneid@cmi.univ-mrs.fr

**Wouter J. T. Bos**

LMFA-CNRS  
Ecole Centrale de Lyon - Université de Lyon  
36 Avenue Guy de Collongues, 69134 Ecully Cedex, France  
wouter.bos@ec-lyon.fr

**Marie Farge**

LMD-IPSL-CNRS  
Ecole Normale Supérieure  
24 rue Lhomond, 75231 Paris Cedex 5, France  
farge@lmd.ens.fr

### ABSTRACT

The acceleration statistics of sheared and rotating homogeneous turbulence are studied using direct numerical simulation results with different rotation ratios of Coriolis parameter to shear rate  $f/S$ . For the range of rotation ratios  $0 \leq f/S \leq 1$ , a destabilization of the flow due to rotation and growth of the turbulent kinetic energy is obtained. For other values of  $f/S$ , rotation stabilizes the flow and a decay of the turbulent kinetic energy is observed. The statistical properties of Lagrangian and Eulerian acceleration are considered and the influence of the rotation ratio and the scale dependence of the statistics is investigated. The probability density functions (pdfs) of both Lagrangian and Eulerian acceleration show a strong and similar dependence on the rotation ratio. The flatness further quantifies its dependence and yields values close to three for strong rotation. For moderate and vanishing rotation, the flatness of the Eulerian acceleration is larger than that of the Lagrangian acceleration, contrary to previous results for isotropic turbulence. A wavelet-based scale-dependent analysis shows that the flatness of both Eulerian and Lagrangian acceleration increases as scale decreases. For strong rotation, the Eulerian acceleration is more intermittent than the Lagrangian acceleration, while the opposite result is obtained for moderate rotation.

### INTRODUCTION

The fluid particle acceleration is of fundamental interest in turbulence ranging from theoretical aspects (e.g. Tsinober, 2001) to the Lagrangian modeling of particle dispersion (e.g. Pope, 1994). Applications include transport and mixing in geophysical flows such as the spreading of pollutants in the atmosphere and oceans. In order to comprehend the fluid particle dynamics, their acceleration is of particular interest. A first prediction of the fluid particle acceleration can be found in the works of Heisenberg (1948) and Yaglom (1949). Since then, both extensive experimental investigations, aided by the development of advanced diagnostics (e.g. La Porta et al., 2001), as well as numerous numerical simulations, enabled by the increasing power of supercomputers, have been performed. For recent reviews on Lagrangian properties of turbulent flows we refer the reader to Toschi and Bodenschatz (2009) and Yeung (2002).

The Lagrangian acceleration  $d\mathbf{u}/dt$  consists of the two Eulerian terms  $\partial\mathbf{u}/\partial t$  and  $\mathbf{u} \cdot \nabla\mathbf{u}$ , where  $\mathbf{u}$  denotes the velocity vector in an Eulerian reference frame. By definition, it is invariant with respect to Galilean transformations. The local acceleration  $\partial\mathbf{u}/\partial t$ , also called Eulerian acceleration and dependent on the reference frame, corresponds to the unsteady rate of change of the velocity vector. The con-

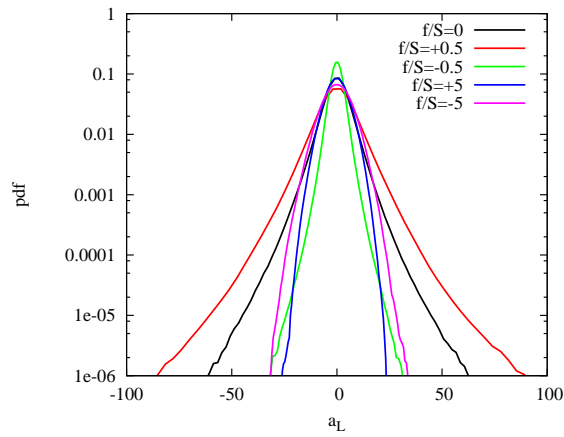


Figure 1. PDFs of Lagrangian acceleration.

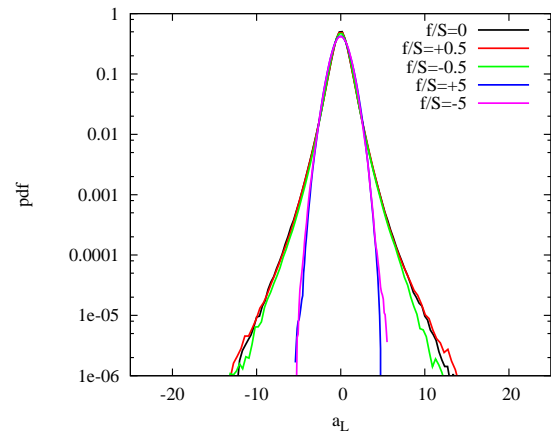


Figure 3. Normalized PDFs of Lagrangian acceleration.

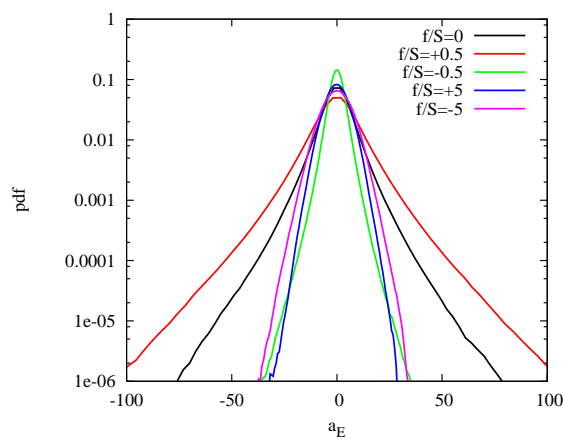


Figure 2. PDFs of Eulerian acceleration.

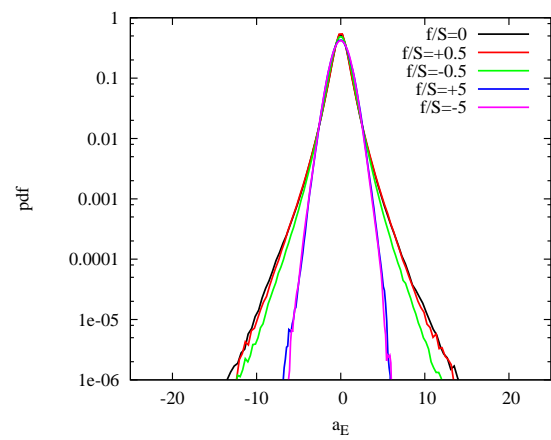


Figure 4. Normalized PDFs of Eulerian acceleration.

vective acceleration  $\mathbf{u} \cdot \nabla \mathbf{u}$  contains effects due to spatial changes of the velocity vector and it includes nonlinear effects.

Considering the incompressible Navier-Stokes equations, the Lagrangian acceleration can be further splitted into an irrotational part, corresponding to the pressure gradient term  $-1/\rho_0 \nabla p$ , and a solenoidal part, corresponding to the viscous dissipation term  $\nu \nabla^2 \mathbf{u}$ . For flows subjected to external body and surface forces, such as the Coriolis force or shear forces, additional terms have to be included and such terms may alter the influence of the pressure gradient term.

For an incompressible Gaussian random velocity field, Holzer and Siggia (1993) have shown that the pressure probability distribution function (pdf) is negatively skewed and has exponential tails. From that purely kinematic result it can be deduced that the pressure gradient term exhibits a Laplace distribution with flatness equal to 6, as confirmed in Yoshimatsu et al. (2009). Hence, exponential tails of the Lagrangian acceleration should not be interpreted as a signature of intermittency, as discussed in Bos et al. (2010) in the context of drift-wave turbulence.

Most studies of acceleration statistics almost exclusively focus on isotropic turbulence (Toschi and Bodenschatz, 2009; Yeung, 2002). It was found that the Lagrangian acceleration exhibits a strong intermittency which is reflected in the heavy tails of the pdfs. For example

in Laporta et al. (2001) it was shown that particles undergo accelerations of up to 1,500 times the acceleration of gravity. Numerical simulations of isotropic turbulence confirmed these results (Toschi and Bodenschatz, 2009). Scale-dependent statistics for turbulent flows using the orthogonal wavelet decomposition have been introduced in Bos et al. (2007) and have been applied to study acceleration statistics for isotropic turbulence in Yoshimatsu et al. (2009). The influence of non-slip walls on the Lagrangian acceleration has been investigated in Kadoch et al. (2008).

The aim of the present work is to study acceleration statistics in turbulent shear flow. We consider here three types of homogeneous shear flows: without rotation, with moderate rotation, and with strong rotation, where the direction of system rotation is either parallel or anti-parallel to the direction of mean vorticity from the shear flow. The direct numerical simulation data discussed in Jacobitz et al. (2008) and Jacobitz et al. (2010) is analyzed to study the statistics of Lagrangian and Eulerian acceleration with a particular focus on the influence of shear and rotation as well as on the scale-dependence of the statistics.

## APPROACH

This study is based on existing direct numerical simulation results of sheared and rotating homogeneous turbulence (Jacobitz et al. 2008; Jacobitz et al. 2010). A de-

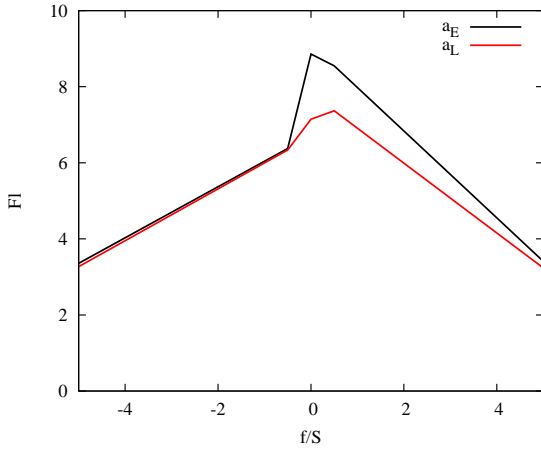


Figure 5. Flatness as a function of  $f/S$ .

composition of the total velocity into a constant mean part  $\mathbf{U} = (U, V, W)$  with

$$U = Sy \quad V = W = 0 \quad (1)$$

leads to the following form of the incompressible Navier-Stokes equations for the fluctuating velocity  $\mathbf{u} = (u, v, w)$ :

$$\nabla \cdot \mathbf{u} = 0 \quad (2)$$

$$\frac{\partial \mathbf{u}}{\partial t} + \mathbf{u} \cdot \nabla \mathbf{u} + Sy \frac{\partial \mathbf{u}}{\partial x} + S v \mathbf{e}_x + 2\boldsymbol{\Omega} \times \mathbf{u} = -\frac{1}{\rho_0} \nabla p + \nu \nabla^2 \mathbf{u} \quad (3)$$

Here,  $S = \partial U / \partial y$  is the constant shear rate,  $f = 2\Omega$  the constant Coriolis parameter for system rotation about the  $y$  coordinate axis,  $\rho_0$  the density, and  $\nu$  the viscosity.

The above equations are transformed into a frame of reference moving with the mean velocity (Rogallo, 1981). This transformation enables the application of periodic boundary conditions for the fluctuating components of velocity and a spectral collocation method is used for the spatial discretization. The solution is advanced in time with a fourth-order Runge-Kutta scheme. The simulations are performed on a parallel computer using  $256 \times 256 \times 256$  grid points. More details about the simulations used in this study can be found in Jacobitz et al. (2008) and Jacobitz et al. (2010).

## RESULTS

The Lagrangian and Eulerian acceleration are defined as

$$\mathbf{a}_L = \frac{\partial \mathbf{u}}{\partial t} + \mathbf{u} \cdot \nabla \mathbf{u} \quad (4)$$

and

$$\mathbf{a}_E = \frac{\partial \mathbf{u}}{\partial t}, \quad (5)$$

respectively. In the following, the accelerations are analyzed at time instant  $St = 5$ . Their properties are studied

for five simulations of sheared and rotating turbulence with rotation ratios of  $f/S = -5, -0.5, 0, +0.5, \text{ and } +5$ . Negative values of  $f/S$  correspond to a parallel configuration and positive values correspond to an anti-parallel configuration between the system rotation and the mean flow vorticity. Isotropic turbulence fields are used to initialize all simulations and the initial values of the Taylor microscale Reynolds number  $Re_\lambda = 45$  and the shear number  $SK/\varepsilon = 2$  are fixed, where  $K$  denotes the turbulent kinetic energy and  $\varepsilon$  its dissipation rate. The evolution of the Taylor microscale Reynolds number depends on the fate of the turbulence and reaches values as high as  $Re_\lambda = 120$ . The shear number varies only weakly with  $f/S$  and assumes a value of about  $SK/\varepsilon = 6$  in the simulations.

The fate of the flows, growth or decay, depends on the value of the rotation ratio  $f/S$ . The non-rotating case with  $f/S = 0$  shows eventual exponential growth of the kinetic energy  $K$ . For moderate rotation ratios, the anti-parallel case with  $f/S = +0.5$  leads to a strong growth of the turbulent kinetic energy, while the parallel case with  $f/S = -0.5$  results in a decay of  $K$ . For strong rotation ratios, however, both the anti-parallel case with  $f/S = +5$  and the parallel case with  $f/S = -5$  lead to a strong decay of  $K$  due to the importance of linear effects.

## Acceleration Statistics

The pdfs of Lagrangian and Eulerian acceleration (estimated using histograms with 100 bins and averaging over the three components) in sheared and rotating turbulence are shown in figures 1 and 2, respectively. A strong and similar dependence on the rotation to shear ratio  $f/S$  is obtained for both accelerations. It is also observed in all cases that the extreme values of the Eulerian acceleration are above those of the Lagrangian acceleration. Figures 3 and 4 present both acceleration pdfs normalized with their corresponding standard deviation. Two families of pdfs are obtained: Gaussian-like behavior for strong rotation  $f/S = \pm 5$  and stretched-exponential-like behavior for the remaining cases.

This influence can be further quantified by considering the flatness of Lagrangian and Eulerian accelerations, defined as the ratio of the fourth order moment divided by the square of the second order moment, as a function of the rotation to shear ratio  $f/S$  (see figure 5). For strong rotation with  $f/S = \pm 5$ , we find flatness values close to 3, which confirms the Gaussian-like behavior. For the remaining cases, larger values are observed for the flatness with a maximum at  $f/S = 0$  for the Eulerian acceleration and  $f/S = +0.5$  for the Lagrangian acceleration. For positive values of  $f/S$ , the flatness of the Eulerian acceleration is clearly larger than the flatness of the Lagrangian acceleration. The difference between the two accelerations decreases with increasing  $f/S$  and for  $f/S = +5$  we find a value close to 3. Contrary to previous results for isotropic turbulence (Ishihara et al., 2007), the Eulerian acceleration pdfs exhibit heavier tails than their Lagrangian counterparts. The fluctuating pressure gradients thus seem to be less important in rotating and sheared turbulence as compared to isotropic turbulence.

## Scale-dependent Analysis

The scale-dependent Lagrangian or Eulerian accelerations are obtained by decomposing the vector  $\mathbf{a} = (a^1, a^2, a^3)$  with  $\mathbf{a} = \mathbf{a}_L$  or  $\mathbf{a}_E$ , respectively, given at resolution  $N = 2^{3J}$  with  $J = 8$ , into an orthogonal wavelet series

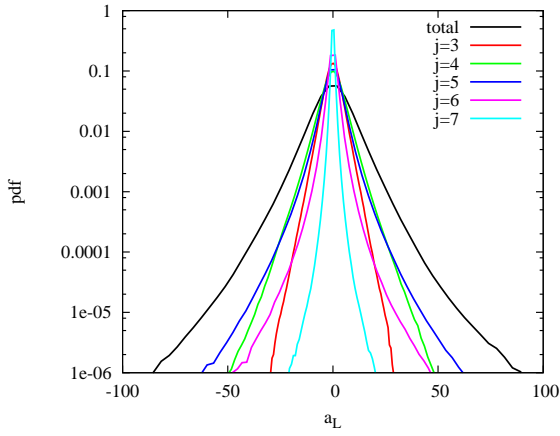


Figure 6. Scale-dependent PDFs of Lagrangian acceleration for  $f/S = +0.5$ .

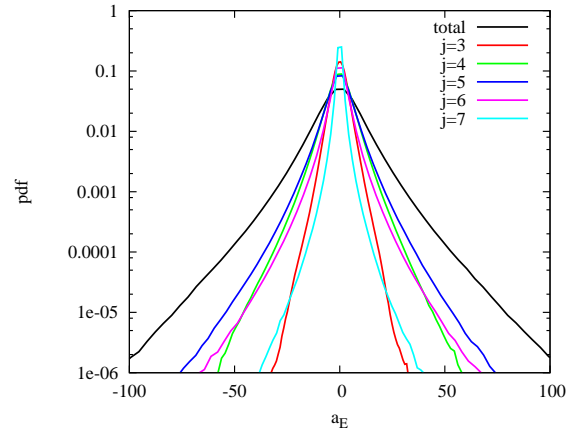


Figure 8. Scale-dependent PDFs of Eulerian acceleration for  $f/S = +0.5$ .

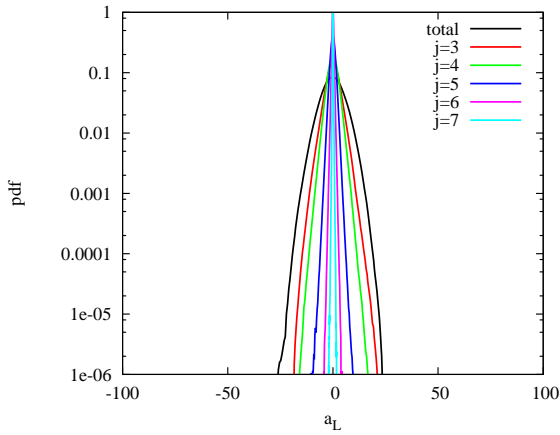


Figure 7. Scale-dependent PDFs of Lagrangian acceleration for  $f/S = +5$ .

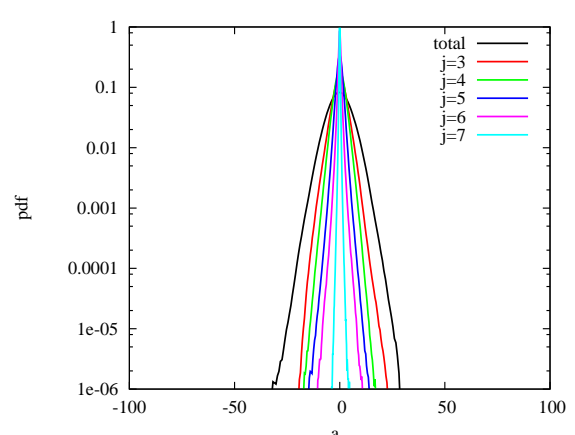


Figure 9. Scale-dependent PDFs of Eulerian acceleration for  $f/S = +5$ .

using Coiflet 12 wavelets

$$\mathbf{a}(\mathbf{x}) = \sum_{\lambda} \tilde{\mathbf{a}}_{\lambda} \psi_{\lambda}(\mathbf{x}) \quad (6)$$

where the multi-index  $\lambda = (j, \mathbf{i}, \mu)$  denotes scale  $j$  (with  $0 \leq j \leq J-1$ ), spatial position  $\mathbf{i}$  (with  $2^{3j}$  values for each  $j$  and  $\mu$ ) and seven spatial directions  $\mu = 1, \dots, 7$  of each wavelet  $\psi_{\lambda}$  (Farge, 1992). Orthogonality implies that the wavelet coefficients are given by  $\tilde{\mathbf{a}}_{\lambda} = \langle \mathbf{a}, \psi_{\lambda} \rangle$ , where  $\langle \cdot, \cdot \rangle$  denotes the  $L^2$ -inner product. The coefficients measure fluctuations of  $\mathbf{a}$  at scale  $2^{-j}$  and around position  $\mathbf{i}/2^j$  for each of the 7 possible directions. Fixing  $j$  and summing only over  $\mathbf{i}$  and  $\mu$ , the contribution of  $\mathbf{a}$  at scale  $j$  is obtained and by construction we have  $\mathbf{a} = \sum_j \mathbf{a}_j$ .

For the wavelet-based scale-dependent analysis, two cases with moderate rotation to shear ratio  $f/S = +0.5$  and strong rotation to shear ratio  $f/S = +5$  are considered. The pdfs of Lagrangian acceleration for  $f/S = +0.5$  and  $f/S = +5$  are shown in figures 6 and 7, respectively. For the growing case with  $f/S = +0.5$ , a stretched-exponential-like behavior is observed at most scales (excluding the largest scales), while the decaying case with  $f/S = +5$  shows Gaussian-like behavior at all scales. The correspond-

ing Eulerian accelerations for cases with  $f/S = +0.5$  and  $f/S = +5$ , presented in figures 8 and 9, respectively, show similar features. However, the tendency for larger extreme values of the Eulerian acceleration observed for the total pdf persists at all scales.

The normalized pdfs of both Lagrangian acceleration, shown in figures 10 and 11, and Eulerian acceleration, shown in figures 12 and 13, vary with scale for the two rotation to shear ratios. With decreasing scale, i.e. increasing scale index  $j$ , the tails become heavier. Again, heavier tails are present at all scales for the case  $f/S = +0.5$  which reflect the stronger intermittency of the flow.

The scale-dependent flatness of both the Lagrangian and Eulerian accelerations for the two  $f/S$  values (see figure 14) shows a strong increase for decreasing scale (increasing  $j$ ). For  $f/S = +0.5$ , the flatness of the Lagrangian acceleration is larger than the flatness of the Eulerian acceleration (for  $j > 4$ ), similar to observations for isotropic turbulence in Yoshimatsu et al. (2009). In the case  $f/S = +5$ , the values of the Eulerian acceleration are larger than the values of the Lagrangian acceleration (for  $j > 4$ ), which must be due to the fact that the effect of the nonlinear term becomes weaker for increasing rotation.

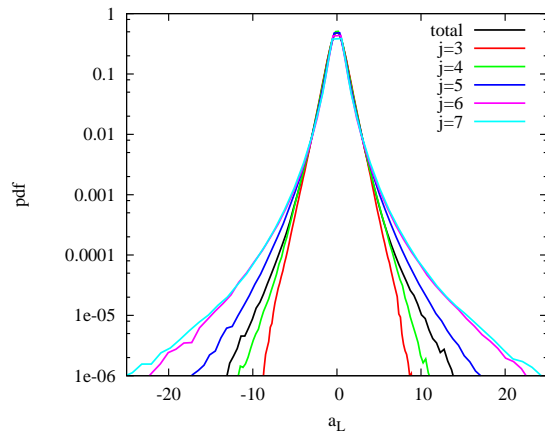


Figure 10. Normalized scale-dependent PDFs of Lagrangian acceleration for  $f/S = +0.5$ .

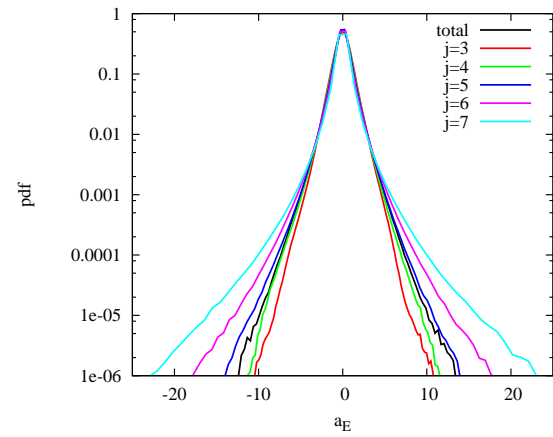


Figure 12. Normalized scale-dependent PDFs of Eulerian acceleration for  $f/S = +0.5$ .

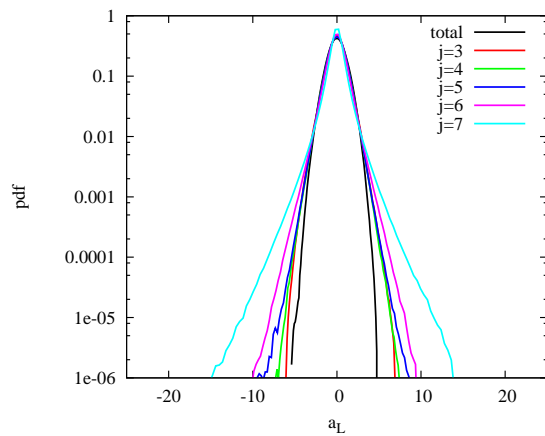


Figure 11. Normalized scale-dependent PDFs of Lagrangian acceleration for  $f/S = +5$ .

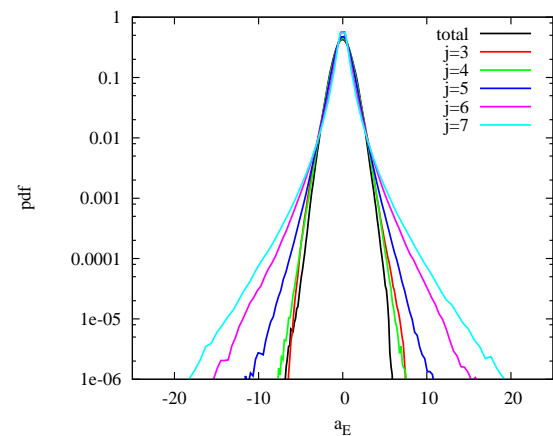


Figure 13. Normalized scale-dependent PDFs of Eulerian acceleration for  $f/S = +5$ .

## CONCLUSIONS

In this study, the acceleration statistics of sheared and rotating homogeneous turbulence are evaluated from direct numerical simulations for a variety of rotation ratios  $f/S$ . The pdfs of both Lagrangian and Eulerian acceleration exhibit a clear dependence on  $f/S$ . For both accelerations, the flatness yields values close to three for strong rotation which indicate a Gaussian-like behavior. For moderate and vanishing rotation, however, the flatness of the Eulerian acceleration is larger than that of the Lagrangian acceleration, contrary to previous results for isotropic turbulence. A wavelet-based scale-dependent analysis shows that the flatness of both Lagrangian and Eulerian accelerations increases as scale decreases. For strong rotation, the Eulerian acceleration is more intermittent than the Lagrangian acceleration, while the opposite result is obtained for moderate rotation.

## ACKNOWLEDGEMENTS

FJ acknowledges support from an International Opportunity Grant from the University of San Diego. WB and KS thankfully acknowledge financial support from the ANR, project SiCoMHD and MF and KS from Euratom-FR-FCM contract No. n2 TT.FR.1215.

## REFERENCES

- Bos, W.J.T., Kadoch, B., Neffaa, S. & Schneider, K. 2010 Lagrangian dynamics of drift wave turbulence. *Physica D* **239**, 1269–1277.
- Bos, W.J.T., Liechtenstein, L. & Schneider, K. 2007 Small-scale intermittency in anisotropic turbulence. *Phys. Rev. E* **76**, 046310.
- Farge, M. 1992 Wavelet transforms and their applications to turbulence. *Annu. Rev. Fluid Mech.* **24**, 395–458.
- Heisenberg, W. 1948 Zur statistischen Theorie der Turbulenz. *Zeitschrift für Physik* **124**, 628–657.
- Holzer, M. & Siggia, E. 1993 Skewed, exponential pressure distributions from Gaussian velocities. *Phys. Fluids A* **5**, 2525.
- Ishihara, T., Kaneda, Y., Yokokawa, M., Itakura, K. & Uno, A. 2007 Small-scale statistics in high-resolution direct numerical simulation of turbulence: Reynolds number dependence of one-point velocity gradient statistics. *J. Fluid Mech.* **592**, 335–366.
- Jacobitz, F.G., Liechtenstein, L., Schneider, K. & Farge, M. 2008 On the structure and dynamics of sheared and rotating turbulence: Direct numerical simulation and wavelet-based coherent vortex extraction. *Phys. Fluids* **20**, 045103.
- Jacobitz, F.G., Schneider, K., Bos, W.J.T. & Farge, M.

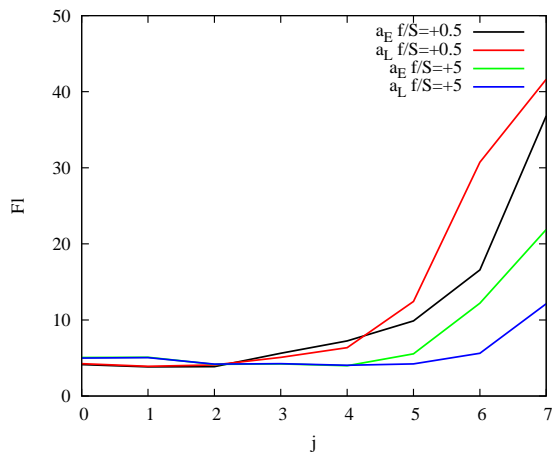


Figure 14. Flatness for  $f/S = 0.5$  and  $5$  as a function of scale.

2010 On the structure and dynamics of sheared and rotating turbulence: Anisotropy properties and geometrical scale-dependent statistics. *Phys. Fluids* **22**, 085101.

Kadoch, B., Bos, W.J.T. & Schneider, K. 2008 Extreme Lagrangian acceleration in confined turbulent flow. *Phys. Rev. Lett.* **100**, 184503.

La Porta, A., Voth, G.A., Crawford, A.M., Alexander, J. & Bodenschatz, E. 2001 Fluid particle accelerations in fully developed turbulence. *Nature* **409**, 1017–1019.

Pope, S.B. 1994 Lagrangian PDF methods for turbulent flows. *Annu. Rev. Fluid Mech.* **26**, 23–63.

Rogallo, R.S. 1981 Numerical experiments in homogeneous turbulence. NASA Technical Memorandum 81315.

Toschi, F. & Bodenschatz, E. 2009 Lagrangian properties of particles in turbulence. *Annu. Rev. Fluid Mech.* **41**, 375–404.

Tsinober, A. 2001 *An informal introduction to turbulence*. Kluwer Academic Publishers.

Yaglom, A.M. 1949 On the acceleration field in a turbulent flow. *C.R. Akad. URSS* **67** 795–798.

Yeung, P.K. 2002 Lagrangian investigations of turbulence. *Annu. Rev. Fluid Mech.* **34**, 115–142.

Yoshimatsu, K., Okamoto, N., Schneider, K., Kaneda, Y. & Farge, M. 2009 Intermittency and scale-dependent statistics in fully developed turbulence. *Phys. Rev. E* **79**, 026303.